European Journal of Radiology xxx (2009) xxx–xxx

Contents lists available at ScienceDirect

European Journal of Radiology

journal homepage: www.elsevier.com/locate/ejrad

Compound analysis of gallstones using dual energy computed tomography—Results in a phantom model

Ralf W. Bauer[a,*], Julian R. Schulz[a], Barbara Zedler[b,1], Thomas G. Graf[c,2], Thomas J. Vogl[a]

[a] Department of Diagnostic and Interventional Radiology, Clinic of the Goethe University Frankfurt, Theodor-Stern-Kai 7, 60596 Frankfurt, Germany
[b] Department of Forensic Medicine, Clinic of the Goethe University Frankfurt, Kennedyallee 104, 60596 Frankfurt, Germany
[c] Siemens AG Healthcare Sector, Computed Tomography, Physics and Applications, Siemensstrasse 1, 91313 Forchheim, Germany

ARTICLE INFO

Article history:
Received 25 April 2009
Received in revised form 3 August 2009
Accepted 3 August 2009

Keywords:
Dual energy computed tomography
Compound analysis
Tissue differentiation
Gallstones
Cholesterol

ABSTRACT

Purpose: The potential of dual energy computed tomography (DECT) for the analysis of gallstone compounds was investigated. The main goal was to find parameters, that can reliably define high percentage (>70%) cholesterol stones without calcium components.
Materials and methods: 35 gallstones were analyzed with DECT using a phantom model. Stone samples were put into specimen containers filled with formalin. Containers were put into a water-filled cylindrical acrylic glass phantom. DECT scans were performed using a tube voltage/current of 140 kV/83 mAs (tube A) and 80 kV/340 mAs (tube B). ROI-measurements to determine CT attenuation of each sector of the stones that had different appearance on the CT images were performed. Finally, semi-quantitative infrared spectroscopy (FTIR) of these sectors was performed for chemical analysis.
Results: ROI-measurements were performed in 45 different sectors in 35 gallstones. Sectors containing >70% of cholesterol and no calcium component ($n = 20$) on FTIR could be identified with 95% sensitivity and 100% specificity on DECT. These sectors showed typical attenuation of -8 ± 4 HU at 80 kV and $+22 \pm 3$ HU at 140 kV. Even the presence of a small calcium component (<10%) hindered the reliable identification of cholesterol components as such.
Conclusion: Dual energy CT allows for reliable identification of gallstones containing a high percentage of cholesterol and no calcium component in this pre-clinical phantom model. Results from *in vivo* or anthropomorphic phantom trials will have to confirm these results. This may enable the identification of patients eligible for non-surgical treatment options in the future.

1. Introduction

Gallstones and their medical consequences represent a relevant cost factor in healthcare systems of Western countries. In Germany, 10.5–24.5% of the female and 4.9–13.1% of the male population are estimated to carry gallstones, and about 170,000 cholecystectomies are performed annually [1]. In the United States of America, gallstone disease causes over 700,000 cholecystectomies per year, which is reflected in the health care budget with annual expenses of 6.5 billion USD [2]. The diagnosis of gallstone disease is usually made by clinical presentation, laboratory constellation, and the proof of stone by imaging modalities (mostly ultrasound, endoscopic retrograde or magnetic resonance cholangio-pancreaticography, or computed tomography). Most of the persons carrying gallstones will never develop symptoms. But if gallstone disease becomes evident – mostly as acute cholecystitis or biliary colic – the therapy is very straight forward: whenever possible, definite cure will be sought by removing stones. However, not every patient is eligible for invasive treatment due to personal risk profiles. Further, surgical treatment bears a certain potential of risk inherent in its invasive nature and required anaesthesia.

For the above reasons, early detection of gallstones, that may be suitable for non-invasive treatment options, has always been of great interest. Established methods are extra-corporal shockwave lithotripsy (ESWL) and pharmacological dissolution therapy with gall acids [3,4] – either alone or in combination – and contact dissolution with methyl tert-butyl ether [5]. Recently, first experiences with ezetimibe could show promising results [6]. However, for successful dissolution the identification of high content cholesterol stones is important, as only these stones seem to show satisfying result [3–13].

* Corresponding author at: Klinikum der Goethe-Universität Frankfurt, Institut für Diagnostische und Interventionelle Radiologie, Haus 23C UG, Theodor-Stern-Kai 7, D-60596 Frankfurt, Germany. Tel.: +49 69 6301 7277; fax: +49 69 6301 7258.
E-mail addresses: ralfwbauer@aol.com (R.W. Bauer), julian.schulz@t-online.de (J.R. Schulz), zedler@em.uni-frankfurt.de (B. Zedler), thomas.gt.graf@siemens.com (T.G. Graf), t.vogl@em.uni-frankfurt.de (T.J. Vogl).
[1] Tel.: +49 69 6301 7551; fax: +49 69 6301 5882.
[2] Tel.: +49 9191 186362; fax: +49 9191 188004.

0720-048X/$ – see front matter © 2009 Elsevier Ireland Ltd. All rights reserved.
doi:10.1016/j.ejrad.2009.08.004

In the past, several authors have described computed tomography (CT) for compound differentiation of gallstones [9,14–22]. Results were inconsistent in terms of reliable differentiation of cholesterol to other components, because confidence intervals overlapped, attenuation thresholds to define a cholesterol stone varied, and scanner settings and methods for chemical analysis differed markedly. Further, regular single source scanners with only one X-ray tube were used and stones were mainly scanned at only one predefined tube voltage. Recently a dual source CT (DSCT) system has become available for clinical routine [23,24]. The possibility to operate both tubes at different potentials (dual energy CT; DECT) has brought the option for material and tissue differentiation into clinical routine [25,26].

In this proof-of-concept study, we investigated the potential of DECT for compound analysis of gallstones in a phantom model under optimized *in vitro* conditions. Findings were compared to semi-quantitative Fourier transform infrared spectroscopy (FTIR), which served as the reference standard for chemical gallstone analysis. The main goal of this study was to define parameters that could reliably define gallstone components with a high content (>70%) of cholesterol and no calcium components ("pure" cholesterol components) on DECT.

2. Materials and methods

2.1. Sample collection and phantom model

This study was approved by the ethic committee of the hospital and in compliance with the declaration of Helsinki. In total, 35 gallstones were analyzed with dual energy computed tomography (DECT) and semi-quantitative Fourier transform infrared spectroscopy (FTIR). The stones were taken from a gallstone collection from the Department of Forensic Medicine of our hospital which was built up for teaching purposes. Samples were collected from autopsies performed at the department over a time span of 2 years. Every sample originated from the gallbladder of a different corpse. The gallstones differed from size, colour, surface, and shape. Right after collection, each sample was put into a separate standard plastic specimen container (length: 5.5 cm, diameter: 3.3 cm) filled with regular 10% formalin solution to prevent stones from drying and rotting. A potential interaction of gallstone components with formalin needs to be considered and might be overcome by storage in native bile or freezing stones after collection. However, with the underlying source of gallstones for this study, this shortcoming was inevitable this time. All stones of this collection were completely anonymous, as no patient related information was documented at the time of collection. Further, the samples for this study were randomly numbered.

In our experimental set-up, the specimen containers were put into a regular cylindrical acrylic glass phantom with a diameter of 20 cm and a length of 30 cm. The phantom was filled with regular drinking water at room temperature. For one scan, six containers were lined up in a row along the *z*-axis. Hence, for 35 samples, in total 6 scans were performed. The phantom was orientated in *x*- and *y*-plane so that the stones were placed in the isocenter of the scanner.

2.2. Dual energy computed tomography physical background and scan protocol

A commercially available dual source CT scanner (Somatom Definition, Siemens Healthcare, Forchheim, Germany) equipped with 2 X-ray tubes (tubes A and B) and 2 detector arrays mounted perpendicularly to each other within the gantry was used for CT analysis. Both tubes can be operated at different potentials at the same time, generating different X-ray spectra (dual energy CT). With this setting, it is possible to scan the very same voxel at the same time at two different spectra. Attenuation depends beside density, and chemical composition also on the X-ray spectrum a material is exposed to an effect that is routinely used for plane film X-ray depending on clinical questions and modality (mammography vs. chest X-ray vs. conventional trauma imaging). On CT, some materials show characteristic changes in CT value (Hounsfield Units; HU) depending on the X-ray spectrum exposed to [27]. Based on this physical background, it is theoretically possible to differentiate between materials and tissues by this so called dual energy effect.

Scans were performed operating the dual source CT system in dual energy mode using a dual energy abdomen protocol with the following settings: tube voltage/current of 140 kV/83 mAs on tube A and 80 kV/340 mAs on tube B, gantry rotation time of 0.5 s, and a pitch of 0.55. As the underlying experiment set-up with a 20 cm water phantom represents a noise optimized condition, a collimation of $2 \times 32 \times 0.6$ mm on both detectors was used for improved spatial resolution and less influence of partial volume averaging. For regular clinical in-patient use a collimation of 14×1.2 mm is recommended by the manufacturer and in recent literature [25], because of higher expected noise and cross scattered radiation.

Three image series were reconstructed, one series each for 80 kV, 140 kV, and one mixed series merging 70% of the 140 kV and 30% of the 80 kV data to generate the impression of a regular 120 kV image. Images were reconstructed at a slice thickness of 0.75 mm with an increment of 0.4 mm and a dedicated medium smooth kernel (D30f) in a standard abdomen window (width 400 HU, center 50 HU). However, for image interpretation, window settings could be freely adjusted for both the 80 kV and 140 kV image series.

2.3. Image interpretation

Dual energy images were analyzed with dedicated software (Syngo workstation, Siemens). Both the 80 kV and the 140 kV series are loaded into the application simultaneously. The software supports a regular 3D view (axial, sagittal, coronal) for the gray scale images and allows to mix the 80 kV and 140 kV data in steps of 1%.

First, stones were simply classified according to their CT patterns by visual impression at both 80 kV and 140 kV as homogenous hypodense, homogenous isodense, homogenous hyperdense, or mixed, if they showed more than one CT pattern—all compared to the surrounding formalin. The maximum diameter of each stone was measured. Then region of interest (ROI) measurements were performed using a circle tool. The software automatically displays the referring CT attenuation (Hounsfield units, HU) for 80 kV and 140 kV, simultaneously. ROI were drawn as large as possible. In homogenous stones, only one ROI was placed. In stones that consisted of various sectors of different densities on CT – e.g. core and shell – ROI measurements were performed separately for every visually identified sector. Further, the attenuation of water and formalin was determined. Beside mean CT number within a ROI also standard deviation (i.e. noise) was recorded. All measurements were performed in axial, sagittal, and coronal plane for each area (i.e. 3 measurements of the same area in total) to minimize the influence of potential measurement errors; thereof, a mean value was calculated, which later statistical analysis was based on.

2.4. Chemical analysis

After DECT phantom scans were completed, the stones were analyzed with Fourier transform infrared spectroscopy (FTIR; IFS 28, Bruker, Karlsruhe, Germany). FTIR spectroscopy is an analogue to regular photometry, but instead of the visible spectrum of light, infrared light is used. The substance to be analyzed is embedded in a ground matrix (potassium bromide–KBr), which is lucent for IR

Please cite this article in press as: Bauer RW, et al. Compound analysis of gallstones using dual energy computed tomography—Results in a phantom model. Eur J Radiol (2009), doi:10.1016/j.ejrad.2009.08.004

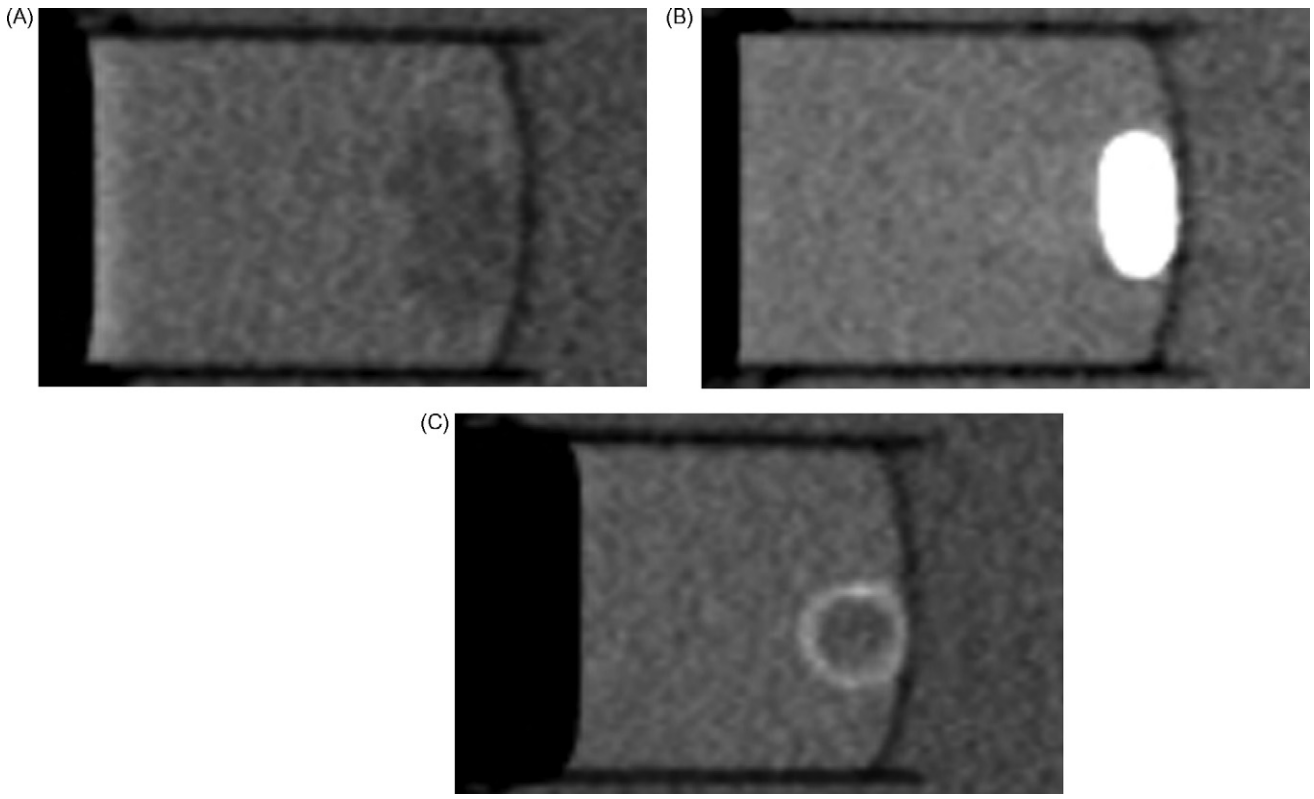

Fig. 1. Stone samples at 80 kV. (A) shows a "pure" cholesterol stone (no. 27) consisting of 90% of cholesterol and 10% of protein. Note the typical hypodense appearance at 80 kV (−12 HU). The stone was not visible at 140 kV (19 HU). In opposite, (B) shows a "non-cholesterol" stone (no. 33), with only 20% of cholesterol and 60% of calcium and the typical hyperdense attenuation (2176/1491 HU at 80/140 kV). (C) shows a stone consisting of shell and core, and therefore of two separate sectors (nos. 15 and 40). While the core showed typical characteristics of "pure" cholesterol with 70% of cholesterol and 30% of protein, the shell was also correctly identified as "non-cholesterol" sector with only 40% of cholesterol and 60% of protein.

light. Afterwards, the sample is exposed to a known IR spectrum and transmission and absorption of certain wavelengths are measured behind the sample. By transmission/absorption characteristics, the substances contained in the sample can be identified.

Preparation of the stones was done with the help of the DECT images. Stones that appeared homogenous on CT were powdered in toto, embedded in the KBr matrix, and analyzed. For stones with more than one component on DECT, each identified sector was analyzed separately. For that, representative parts of the stones were cut or scratched off with a scalpel as accurately as possible in concordance with the DECT images.

FTIR spectroscopy measurements were allocated and verified with the help of computer-based libraries for reference spectra. Results were displayed semi-quantitatively: stone composition could be described in steps of ten percent.

As only gallstones with a high percentage of cholesterol and without major calcification seem to show good results with dissolution therapy, the main goal of this work was to find criteria for the reliable identification of such pure cholesterol compounds on DECT. We constituted a threshold of 70% of cholesterol and no calcium compound to define "pure" cholesterol on FTIR, whereas less than 70% of cholesterol or the presence of any percentage of calcium defined "non-cholesterol" sectors [28].

2.5. Statistical analysis

Dedicated software was used for statistical analysis (BiAS 8.4, Epsilon, Frankfurt, Germany). Mean ± standard deviation was calculated for the measured CT attenuations and compared using the Wilcoxon–Mann–Whitney-*U* test. The corresponding CT values for 80 kV and 140 kV were plotted in a scattergram. Based on the attenuation measurements, sensitivity and specificity were calculated for DECT compared to FTIR to detect gallstone components with a high content (>70%) of cholesterol and no calcium components ("pure" cholesterol components).

3. Results

The mean attenuation of formalin was determined to be 16 ± 2 HU with a standard deviation (SD) (i.e. noise) measured within the ROI of 12 ± 1 HU at 80 kV and 15 ± 2 HU with a SD of 10 ± 1 HU at 140 kV. Water showed attenuation of −5 ± 0 HU with a SD of 13 ± 0 HU at 80 kV and −4 ± 0 HU and a SD of 12 ± 0 HU at 140 kV. CTDIvol was 17.8 mGy.

Of total 35 stones, 12 were not visible at 140 kV regardless of window settings, but all stones were visible at 80 kV. Because of that phenomenon, further analysis and ROI measurements were based on the 80 kV image series. At 80 kV, 25 stones showed homogenous attenuation ($n = 13$ hyperdense, $n = 12$ hypodense), whereas in 10 stones shell and core could be differentiated (7 stones with hypodense core and hyperdense shell, 3 stones with hyperdense core and more hyperdense shell) (Fig. 1). Following that, ROI measurements were performed in totally 45 sectors. Results were plotted in a diagram (Fig. 2). Mean stone diameter was 1.3 cm (range 0.4–2.4 cm). The smallest single sector that was measured was a 2 mm thick hyperdense shell; the referring ROI had a size of 3 mm^2. The smallest homogenous hyperdense and hypodense stones that were measured had a diameter of 4 mm and 5 mm with a size of the referring ROI of 17 mm^2 and 20 mm^2, respectively. All 19 sectors that appeared hypodense at 80 kV and were invisible at 140 kV were grouped in the lower left part of the curve and showed slightly negative attenuation values at 80 kV (−1 to −15 HU) and positive

Please cite this article in press as: Bauer RW, et al. Compound analysis of gallstones using dual energy computed tomography—Results in a phantom model. Eur J Radiol (2009), doi:10.1016/j.ejrad.2009.08.004

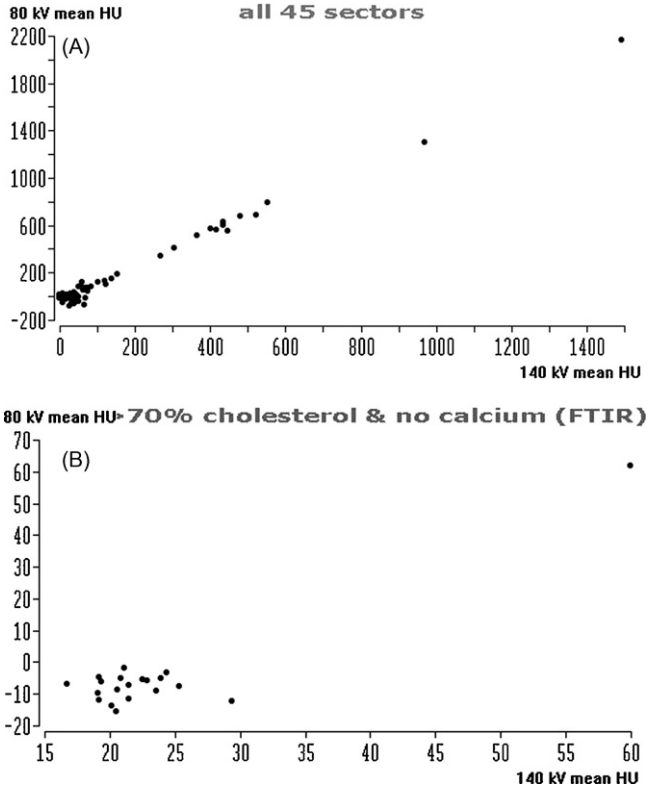

Fig. 2. Dual energy characteristics. The dual energy characteristics, i.e. attenuation at 80 kV and 140 kV, of each of the 45 measured stone sectors are plotted in the diagram of Fig. A. Fig. B displays all sectors that were classified as "pure" cholesterol by FTIR spectroscopy. Note that 19 of them show negative values at 80 kV and positive values at 140 kV. These sectors were correctly identified as "pure" cholesterol by DECT.

attenuation values at 140 kV (+17 to +29 HU).

On FTIR spectroscopy, identified stone components for the 45 sectors were cholesterol, bilirubin, protein, carbonates, and phosphates. The carbonates turned out to be modifications of calcium carbonate. Phosphates were accompanied with calcium as counter ion as well. Based on that, FTIR spectroscopy determined 20 sectors with >70% of cholesterol and no calcium compound and 25 sectors with either <70% of cholesterol or any calcium compound. DECT recognized 19 out of these 20 sectors with certain characteristics of attenuation: Every sector showed slightly negative attenuation at 80 kV (mean -8 ± 4 HU, range -15 to -1 HU, with a SD (i.e. noise) within the ROI of 12 ± 2 HU) and positive attenuation at 140 kV (mean 22 ± 3 HU, range 17–29 HU, with a SD within the ROI of 11 ± 2 HU). Attenuation at both, 80 kV and 140 kV was significantly different from that of formalin and water ($p < 0.001$), whereas noise was not ($p > 0.9$). These 19 sectors showed the above mentioned phenomenon, that they were visible at 80 kV and invisible at 140 kV. In contrast, 25 of the 26 sectors that were visible at 140 kV contained somewhat amount of calcium or less than 70% of cholesterol. Table 1 provides a detailed overview of the results obtained by DECT and FTIR spectroscopy.

Thus, DECT could differentiate 44 out of 45 measurements correctly: 19 as being "pure" cholesterol sectors (true positive) and another 25 as being "non-cholesterol" sectors (true negative). Based on these values, we determined a sensitivity of 95% and specificity of 100% for DECT compared to FTIR spectroscopy to differentiate between "pure cholesterol" and "non-cholesterol" sectors (Table 2).

The attenuation values of the 25 sectors that were classified as "non-cholesterol" sectors by FTIR spectroscopy ranged from 26 HU to 2176 HU at 80 kV (mean 429 ± 478 HU) and from 40 HU to 1491 HU at 140 kV (mean 315 ± 328 HU) and were significantly higher than the attenuation of "pure" cholesterol sectors ($p < 0.001$), and there was no overlap of attenuation values, neither at 80 kV, nor at 140 kV. Likewise, sectors with >70% cholesterol but with up to 10% calcium ($n = 5/25$) also showed significantly ($p < 0.001$) higher attenuation values than "pure" cholesterol sectors (80 kV: mean 241 ± 195 HU, range 26–520 HU; 140 kV: mean 186 ± 129 HU, range 40–364 HU), also with no overlap.

4. Discussion

Predicting the composition of gallstones by CT has been widely explored in the past. To our knowledge, these studies were mostly based on single source CT using only one predefined tube potential [7,9,12,14–18,20–22,29]. Inverse correlation between stone density and cholesterol content could be demonstrated. But especially attenuation threshold for cholesterol largely diversified in these studies ranging from 50 HU to 140 HU, and showed a relevant overlap with other stone components [9,15,17,18,20,22]. In this study we found out that with DECT it is possible to circumscribe attenuation for cholesterol gallstones without a wide diversity. Restricting CT numbers from -1 to -15 HU at 80 kV and from +17 to +29 HU at 140 kV, we defined stone components with >70% of cholesterol and no calcium under *in vitro* conditions. These values allow the detection of "pure" cholesterol components of gallstones (>70% of cholesterol and no calcium) with a sensitivity of 95% and enable the differentiation to "non-cholesterol" stone components with a specificity of 100%. As we have also shown, the detection of gallstones with >70% of cholesterol is limited to the fact that even a small percentage of calcium components (1–10%) influences attenuation significantly, and it was not possible to detect them with DECT as being cholesterol components in this study.

The core of stone 1 showed hyperdense attenuation around 60 HU at both tube voltages and was therefore not identified as cholesterol sector on DECT. But spectroscopy revealed a composition of 80% cholesterol, 10% protein, 10% of bilirubin, and no calcium compound (false negative). Assuming that both DECT and FTIR measurements were correct, no reliable explanation for this finding can be given. A significant influence of bilirubin seems to be unlikely, as stone 3 consisted of 20% bilirubin with 70% cholesterol and was correctly classified as cholesterol stone. In general, the observed results led us to the conclusion that the presence and ratio of cholesterol and calcium compounds strongly affect attenuation characteristics on DECT. For example, the shell of stone 19 showed non-cholesterol characteristics, although containing only 10% of calcium but 80% of cholesterol (Table 1). Vice versa, stone 32 offered no cholesterol and no calcium compounds on FTIR spectroscopy, but could also be successfully classified as a non-cholesterol stone (Table 1). Showing both conditions, containing no cholesterol, but 40% of calcium, stone 12 resulted in higher attenuation values than the shell of stone 19 (sector no. 19-2) and 32 (Table 1). In this context, proteins and bilirubin do not seem to have significant influence on the appearance of gallstone on DECT.

Gallstone disease concerns abdominal medicine day by day. Associated with evaluated risk factors like body mass index (BMI), increasing age, diabetes, high triglyceride, and low HDL cholesterol [30], the incidence of gallstones is rising among an ageing population and upcoming metabolic syndrome [31]. Imaging the stone is important to ensure diagnosis, and comparisons between different imaging modalities have been drawn. Although CT is significantly superior to plane film X-ray and seems to be on par with US in the detection of gallstones [32], not every stone is detected by single source single energy CT. This may be due to the fact, that the standard default tube voltage for most of the CT protocols in adults is 120 kV, and that this X-ray spectrum may not be suitable to detect "pure" cholesterol stones. In this study, 19 of 20 "pure" cholesterol

Please cite this article in press as: Bauer RW, et al. Compound analysis of gallstones using dual energy computed tomography—Results in a phantom model. Eur J Radiol (2009), doi:10.1016/j.ejrad.2009.08.004

Table 1
Results DECT and FTIR analysis.

Sector	DECT		FTIR				Visibility	Stats			
	80 kV	140 kV	Chol	Ca++	Protein	Bilirubin	140 kV	TP	TN	FP	FN
1	62	60	80	0	10	10	+				×
2	−1	21	90	0	10	0		×			
3	−8	25	70	0	10	20		×			
4	−7	17	90	0	10	0		×			
5	−6	23	90	0	10	0		×			
6	−6	19	70	0	30	0		×			
7	−5	21	70	0	30	0		×			
8	−5	22	90	0	10	0		×			
9	−13	20	80	0	20	0		×			
10	−7	21	90	0	10	0		×			
11	63	66	30	0	40	30	+		×		
12	558	444	0	40	30	30	+		×		
13	−9	21	90	0	10	0		×			
14	84	81	40	0	20	40	+		×		
15	−11	21	70	0	30	0		×			
16	695	519	50	30	20	0	+		×		
17	679	478	0	20	70	10	+		×		
18	70	61	30	10	40	20	+		×		
19	−3	24	80	0	20	0		×			
20	−9	24	80	0	20	0		×			
21	152	135	0	0	70	30	+		×		
22	−5	19	80	0	20	0		×			
23	53	65	10	0	40	50	+		×		
24	1306	969	0	10	70	20	+		×		
25	569	414	0	70	0	30	+		×		
26	26	40	80	10	10	0	+		×		
27	−12	19	90	0	10	0		×			
28	520	364	80	10	10	0	+		×		
29	−12	29	80	0	20	0		×			
30	−15	20	80	0	20	0		×			
31	639	433	70	20	10	0	+		×		
32	134	118	0	0	90	10	+		×		
33	2176	1491	20	60	10	10	+		×		
34	−10	19	80	0	20	0		×			
35	−5	24	70	0	20	0		×			
36 (1-2)	192	152	80	10	10	0	+		×		
37 (5-2)	79	75	50	0	40	10	+		×		
38 (8-2)	131	101	70	20	10	0	+		×		
39 (10-2)	121	106	80	10	10	0	+		×		
40 (15-2)	87	76	40	0	60	0	+		×		
41 (18-2)	797	551	0	70	10	20	+		×		
42 (19-2)	346	267	80	10	10	0	+		×		
43 (26-2)	418	304	60	20	20	0	+		×		
44 (29-2)	577	400	60	10	30	0	+		×		
45 (35-2)	618	433	60	20	0	20	+		×		
Sum							26	19	25	0	1

Detailed overview on every analyzed gallstone sector: mean attenuation at 80 kV and 140 kV on dual energy computed tomography (DECT) in Hounsfield Units (HU), results of semi-quantitative Fourier transform infrared spectroscopy (FTIR) in percent (%), visibility on the 140 kV image series, and the basis for the calculation of sensitivity and specificity (TP = true positive, TN = true negative, FP = false positive, FN = false negative) are provided.

sectors were only visible at 80 kV and could not be delineated at 140 kV regardless of window settings.

With CT, many authors especially focussed on the detection of cholesterol in order to change therapy for affected patients [7–10,12,16,17,22]. Although nowadays the therapy of choice is cholecystectomy, symptomatic patients who refuse surgery or show a contraindication to surgery or anaesthesia are to be treated with therapeutical alternatives (oral gall acids, extracorporeal shockwave lithotripsy, contact litholysis, ezetimibe) [3–6,11,13,29]. The above mentioned studies have described a correlation between low CT numbers and gallstone clearance, arising thereby that these options demand non- or only low-calcified, high content cholesterol stones for a successful therapy.

Dual source CT (DSCT) with the option of operating both tubes in dual energy mode offers unseen perspectives compared to single energy CT regarding material differentiation in clinical routine: different authors have successfully applied DECT for the differentiation of urinary tract stones (uric acid from calcified stones) [33–36] and the detection of iodinated contrast material in different tissues of the body [37–40]. The dual energy technique is based on the fact that attenuation of different materials and tissues varies with the tube potential, and therefore X-ray spectrum, they are scanned with. The spread and ratio of attenuation values at a high and low tube voltage – and therefore the dual energy effect – depend on effective atomic number and will expand with a bigger difference in X-ray spectrum to a certain point and can be characteristic for certain materials and tissues [27]. However, as for clinical routine use compromises need to be made in terms of image noise and applied dose, a tube voltage of 140 kV and 80 kV on tubes A and B, respectively, is used for most clinical DECT applications, so far.

Different tube potential settings with single source CT have been tested for gallstone differentiation in the past. Chan et al. [19] scanned gallstones *in vitro* with voltages of 80 kV, 100 kV, 120 kV, and 140 kV, separately, and found the detection rate of gallstones at 140 kV to be the highest. They further described a relevant overlap of CT values of cholesterol and pigment stones, so that a reliable identification was not possible in every case, although cholesterol showed lower attenuation at 80 kV than at 140 kV—like

Please cite this article in press as: Bauer RW, et al. Compound analysis of gallstones using dual energy computed tomography—Results in a phantom model. Eur J Radiol (2009), doi:10.1016/j.ejrad.2009.08.004

Table 2
Sensitivity and specificity DECT vs. FTIR.

		FTIR		
		Positive	Negative	Sum
DECT	Positive	19	0	19
	Negative	1	25	26
	Sum	20	25	45
	Sensitivity	19/(19 + 1) = 95%		
	Specificity	25/(25 + 0) = 100%		

Based on the results from Table 1 a sensitivity of 95% and a specificity of 100% were calculated for dual energy computed tomography (DECT) compared to Fourier transform infrared spectroscopy (FTIR) for the correct detection of "pure" cholesterol sectors with >70% of cholesterol and no calcium compound.

in our study. The discrepancy with our findings may be explained by some substantial differences to our study concept. First, on FTIR spectroscopy stones were analyzed in toto and not sectorwise—a core/shell appearance on CT was not considered for chemical analysis. Further, stones were classified only according to their main component into cholesterol ($n = 71$) and pigment ($n = 15$) stones. No quantitative analysis was performed, and no information was given about the amount of calcium compounds and how they affected CT density. Second, only a single ROI per stone was placed on CT images encompassing as much of the stone as possible on 5 mm thick slices. This limits spatial resolution and average areas of different density and therefore does not differentiate between areas of different chemical composition. Altogether, this may explain the overlap and wide range of CT values of cholesterol and pigment stones. Third, stones were put into NaCl solution for phantom measurements which has been shown to significantly alter attenuation values of gallstone components compared to measurement in native bile, more than formalin [41]. Further, no information was given how CT values of saline solution at the different kV settings changed. However, the density characteristic of NaCl seems to be very similar to that of water [27]. Based on our results, cholesterol shows somewhat water-like density only at 80 kV, thus leading to higher absolute contrast between cholesterol and NaCl at 140 kV than at 80 kV. This might account for the finding, that gallstone detection rate was significantly higher at 140 kV than at 80 kV.

Recently, Voit et al. [42] reported their initial results for gallstone differentiation with the same dual energy scanner as in our study. Forty-three gallstones (13 cholesterol stones) were embedded in ultrasound gel and scanned at 80 kV and 140 kV. While analysis of only the gray scale images by two observers showed a poor sensitivity of 54% with a good specificity of 85–89% for the correct classification of the 13 cholesterol stones, colour-coding of HU differences within the stones improved sensitivity and specificity to 100%. Unfortunately, no mean CT numbers and ranges were given for stone components in the paper. The main limitation of the study was that stone differentiation was only performed according to visual criteria by one pathologist. No chemical analysis was done.

4.1. Study limitations

Our study has some limitations that have to be considered. First, 35 stones and 45 measurements represent a small sample size. A larger amount of stones could provide more precise values for sensitivity and specificity. Second, test conditions were optimized in an *in vitro* set-up with a small phantom diameter of only 20 cm and therefore a noise-optimized setting. This allowed us to use a thin collimation of 32×0.6 mm with reconstruction of 0.75 mm slices for improved spatial resolution, whereas for patient use a collimation of 14×1.2 mm is recommended by the manufacturer and in literature [25] to compensate for higher noise. *In vivo* conditions – especially the influence of the patient's body habitus and increased image noise in large patients – have not been examined yet. In this context, radiation dose also has to be considered. The CTDIvol of our scans was 17.8 mGy. We did not change recommended tube current settings of 83 mAs (140 kV) and 340 mAs (80 kV). This was seen as a compromise between the use of a small phantom (which would allow for reduction of tube current) and a thin 0.6 mm collimation (which would require an increase in tube current). It needs to be discussed if in an anthropomorphic phantom also a thin collimation can be applied, how dose and image quality would differ from a thick collimation protocol, and further to what level dose can be reduced to still guarantee diagnostic image quality for *in vivo* use. Third, formalin could possibly influence the CT attenuation of gallstones, even though stone storage in formalin seems to have the least effect on changes in CT value besides storage in native bile [41]. The use of frozen stones for further trials needs to be considered, as a potential interaction of conservation fluids with stone components can be eliminated that way. Fourth, the way samples for FTIR analysis were generated, may be another source of error: Unfortunately it is not guaranteed that the region of the stone that was measured in the DECT images exactly agreed with the particles cut off the stone and analyzed in laboratory. However, to our knowledge only two prior studies also tried to differentiate and analyze regions of different appearance on CT separately [15,18]. However, we think this represents the right approach for the most exact differentiation of stone components. It appears only logical, that areas of different densities on CT have different chemical compositions. Averaging back a high resolution CT image with placing only one ROI would be against the sense of this study, whose purpose was to determine stone components as exactly as possible.

5. Conclusion

In this study we were able to show that compound analysis of gallstones with dual energy CT is feasible. Compared to chemical analysis with infrared spectroscopy serving as reference standard we were able to precisely describe characteristic CT numbers for high-percent cholesterol sectors without calcium components at 80 kV and 140 kV and to detect these sectors with 95% sensitivity and 100% specificity. However, recognizing the above mentioned limits of this study, our results from this phantom trial under optimized conditions may serve following investigations as reference. *In vitro* studies with anthropomorphic phantoms or better *in vivo* trials are needed to clarify the value of our findings and their reproducibility for clinical routine use.

References

[1] Gleisberg C, Bauer H, Fellmann E, et al. Cholezystektomie. Web site of Bundesgeschäftsstelle Qualitätssicherung GGmbH. http://info.bqs-online.de/outcome/12n1/Buaw-2002-12n1-qr.pdf. Published 2002. Updated October 2003. Accessed October 20, 2008.
[2] Shaffer EA. Gallstone disease: epidemiology of gallbladder stone disease. Best Pract Res Clin Gastroenterol 2006;20(6):981–96.
[3] Carrilho-Ribeiro L, Pinto-Correia A, Velosa J, Carneiro De Moura M. A ten-year prospective study on gallbladder stone recurrence after successful extracorporeal shock-wave lithotripsy. Scand J Gastroenterol 2006;41(3):338–42.
[4] Rabenstein T, Radespiel-Troger M, Hopfner L, et al. Ten years experience with piezoelectric extracorporeal shockwave lithotripsy of gallbladder stones. Eur J Gastroenterol Hepatol 2005;17(6):629–39.
[5] Hellstern A, Leuschner U, Benjaminov A, et al. Dissolution of gallbladder stones with methyl tert-butyl ether and stone recurrence: a European survey. Dig Dis Sci 1998;43(5):911–20.
[6] Wang HH, Portincasa P, Mendez-Sanchez N, Uribe M, Wang DQ. Effect of ezetimibe on the prevention and dissolution of cholesterol gallstones. Gastroenterology 2008;134(7):2101–10.
[7] Caroli A, Del Favero G, Di Mario F, et al. Computed tomography in predicting gall stone solubility: a prospective trial. Gut 1992;33(5):698–700.

Please cite this article in press as: Bauer RW, et al. Compound analysis of gallstones using dual energy computed tomography—Results in a phantom model. Eur J Radiol (2009), doi:10.1016/j.ejrad.2009.08.004

[8] Fu XB, Liu JY, Liu GN, Shao XM, Zhou XS. Computed tomography in predicting the efficacy of oral cholelitholysis with bile acids. Chin Med J (Engl) 1993;106(10):734–8.
[9] Hickman MS, Schwesinger WH, Bova JD, Kurtin WE. Computed tomographic analysis of gallstones. An *in vitro* study. Arch Surg 1986;121(3):289–91.
[10] Pereira SP, Veysey MJ, Kennedy C, Hussaini SH, Murphy GM, Dowling RH. Gallstone dissolution with oral bile acid therapy. Importance of pretreatment CT scanning and reasons for nonresponse. Dig Dis Sci 1997;42(8):1775–82.
[11] Petroni ML, Jazrawi RP, Pazzi P, et al. Ursodeoxycholic acid alone or with chenodeoxycholic acid for dissolution of cholesterol gallstones: a randomized multicentre trial. The British-Italian Gallstone Study group. Aliment Pharmacol Ther 2001;15(1):123–8.
[12] Polverosi R, Sbeghen R, Zambelli C, Caracciolo F, Spigariol F, Caroli A. Role of computerized tomography in the densitometric assessment of lithiasis of the gallbladder. Radiol Med 1992;84(4):387–92.
[13] Tuncer I, Harman M, Mercan R, et al. The effects of ursodeoxycholic acid alone and ursodeoxycholic acid plus low-dose acetylsalicylic acid on radiolucent gallstones. Turk J Gastroenterol 2003;14(2):91–6.
[14] Barakos JA, Ralls PW, Lapin SA, et al. Cholelithiasis: evaluation with CT. Radiology 1987;162(2):415–8.
[15] Baron RL, Rohrmann Jr CA, Lee SP, Shuman WP, Teefey SA. CT evaluation of gallstones *in vitro*: correlation with chemical analysis. AJR Am J Roentgenol 1988;151(6):1123–8.
[16] Bell GD, Dowling RH, Whitney B, Sutor DJ. The value of radiology in predicting gallstone type when selecting patients for medical treatment. Gut 1975;16(5):359–64.
[17] Brakel K, Lameris JS, Nijs HG, Terpstra OT, Steen G, Blijenberg BC. Predicting gallstone composition with CT: *in vivo* and *in vitro* analysis. Radiology 1990;174(2):337–41.
[18] Brink JA, Kammer B, Mueller PR, Balfe DM, Prien EL, Ferrucci JT. Prediction of gallstone composition: synthesis of CT and radiographic features *in vitro*. Radiology 1994;190(1):69–75.
[19] Chan WC, Joe BN, Coakley FV, et al. Gallstone detection at CT *in vitro*: effect of peak voltage setting. Radiology 2006;241(2):546–53.
[20] Janowitz P, Zoller A, Swobodnik W, Wechsler JG, Schumacher KA, Ditschuneit H. Computed tomography evaluation of radiolucent gallstones *in vivo*. Gastrointest Radiol 1990;15(1):58–60.
[21] Moss AA, Filly RA, Way LW. *In vitro* investigation of gallstones with computed tomography. J Comput Assist Tomogr 1980;4(6):827–31.
[22] Rambow A, Staritz M, Wosiewitz U, Mildenburger P, Thelen M, Meyer zum Buschenfelde KH. Analysis of radiolucent gallstones by computed tomography for *in vivo* estimation of stone components. Eur J Clin Invest 1990;20(4):475–8.
[23] Flohr TG, McCollough CH, Bruder H, et al. First performance evaluation of a dual-source CT (DSCT) system. Eur Radiol 2006;16(2):256–68.
[24] Johnson TR, Nikolaou K, Wintersperger BJ, et al. Dual-source CT cardiac imaging: initial experience. Eur Radiol 2006;16(7):1409–15.
[25] Graser A, Johnson TR, Chandarana H, Macari M. Dual energy CT: preliminary observations and potential clinical applications in the abdomen. Eur Radiol 2009;19(1):13–23.
[26] Johnson TR, Krauss B, Sedlmair M, et al. Material differentiation by dual energy CT: initial experience. Eur Radiol 2007;17(6):1510–7.
[27] Zatz L. The effect of the kVp level on EMI values. Radiology 1976;119:683–8.
[28] Kim IS, Myung SJ, Lee SS, Lee SK, Kim MH. Classification and nomenclature of gallstones revisited. Yonsei Med J 2003;44(4):561–70.
[29] Sarva RP, Farivar S, Fromm H, Poller W. Study of the sensitivity and specificity of computerized tomography in the detection of calcified gallstones which appears radiolucent by conventional roentgenography. Gastrointest Radiol 1981;6(2):165–7.
[30] Festi D, Dormi A, Capodicasa S, et al. Incidence of gallstone disease in Italy: results from a multicenter, population-based Italian study (the MICOL project). World J Gastroenterol 2008;14(34):5282–9.
[31] Lammert F, Miquel JF. Gallstone disease: from genes to evidence-based therapy. J Hepatol 2008;48(Suppl. 1):S124–35.
[32] Pickuth D, Spielmann RP. Detection of choledocholithiasis: comparison of unenhanced spiral CT, US, and ERCP. Hepatogastroenterology 2000;47(36):1514–7.
[33] Graser A, Johnson TR, Bader M, et al. Dual energy CT characterization of urinary calculi: initial *in vitro* and clinical experience. Invest Radiol 2008;43(2):112–9.
[34] Matlaga BR, Kawamoto S, Fishman E. Dual source computed tomography: a novel technique to determine stone composition. Urology 2008;72(5):1164–8.
[35] Primak AN, Fletcher JG, Vrtiska TJ, et al. Noninvasive differentiation of uric acid versus non-uric acid kidney stones using dual-energy CT. Acad Radiol 2007;14(12):1441–7.
[36] Stolzmann P, Scheffel H, Rentsch K, et al. Dual-energy computed tomography for the differentiation of uric acid stones: ex vivo performance evaluation. Urol Res 2008;36(3–4):133–8.
[37] Fink C, Johnson TR, Michaely HJ, et al. Dual-energy CT angiography of the lung in patients with suspected pulmonary embolism: initial results. Rofo 2008;180(10):873–9.
[38] Pontana F, Faivre JB, Remy-Jardin M, et al. Lung perfusion with dual-energy multidetector-row CT (MDCT): feasibility for the evaluation of acute pulmonary embolism in 117 consecutive patients. Acad Radiol 2008;15(12):1494–504.
[39] Ruzsics B, Lee H, Zwerner PL, Gebregziabher M, Costello P, Schoepf UJ. Dual-energy CT of the heart for diagnosing coronary artery stenosis and myocardial ischemia-initial experience. Eur Radiol 2008;18(11):2414–24.
[40] Thieme SF, Becker CR, Hacker M, Nikolaou K, Reiser MF, Johnson TR. Dual energy CT for the assessment of lung perfusion-correlation to scintigraphy. Eur J Radiol 2008;68(3):369–74.
[41] Schulte SJ, Baron RL. The effect of storage on the computed tomography attenuation of gallstones. Invest Radiol 1994;29(3):307–12.
[42] Voit H, Krauss B, Heinrich MC, et al. Dual-source CT: *in vitro* characterization of gallstones using dual energy analysis. Rofo 2009;181(4):367–73.

Please cite this article in press as: Bauer RW, et al. Compound analysis of gallstones using dual energy computed tomography—Results in a phantom model. Eur J Radiol (2009), doi:10.1016/j.ejrad.2009.08.004